

Change Detection in Precision Manufacturing Processes under Transient Conditions

Zimo (Robin) Wang, Satish T.S. Bukkapatnam

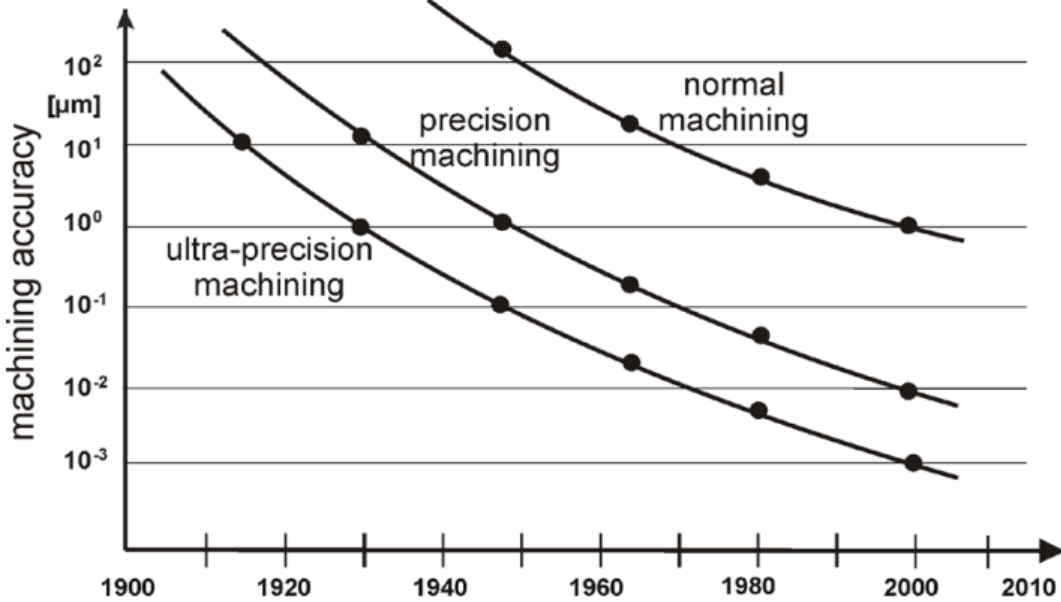
School of Industrial Engineering and Management,
Oklahoma State University

Outline

- Introduction of change detection in precision manufacturing processes
- Change detection in UPM & CMP
- DPGSM-based detection in sensor-based monitoring system during precision manufacturing
- Conclusions

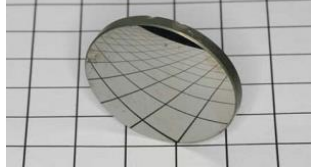
Introduction

- Ultra-Precision Machining (UPM)



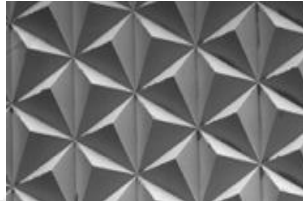
Ultra-precision machining are those technologies by which the highest possible dimensional accuracy is, or has been achieved (Taniguchi, 1983)

Aspheric IR optics

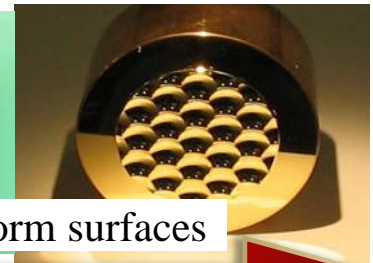


Off-axis Mirrors

Triangular microprisms



Freeform surfaces



1960

1970

1980

1990

2000

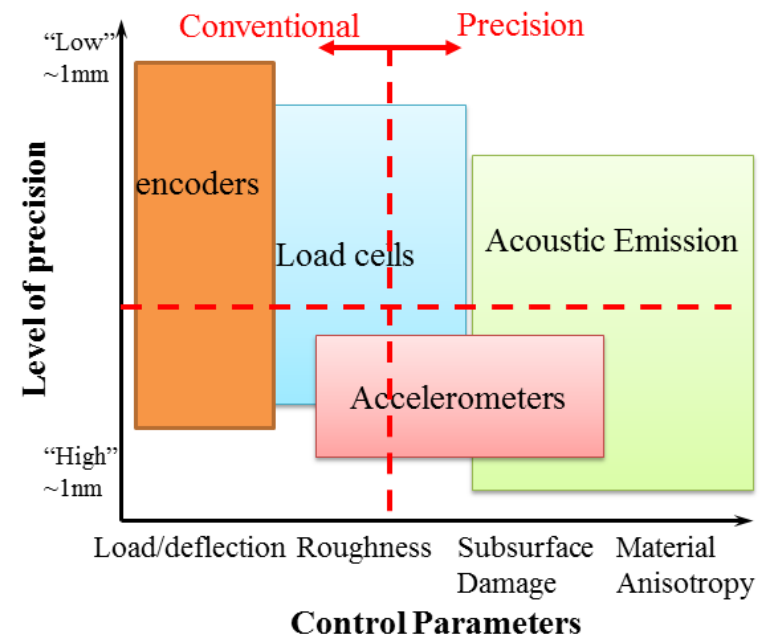
2010

Introduction

- Challenges for UPM quality assurance
 - Limited metrology and methodology for quality control (Dornfeld, 2006)
 - Sensor-based in-process monitoring system of process monitoring and quality control (Abellan-Nebot, 2010)

Demand

- **Suitable sensor based monitoring system for precision machining processes**
- **Effective incipient change detection analyzing weak signal of UPM compared with conventional machining processes**

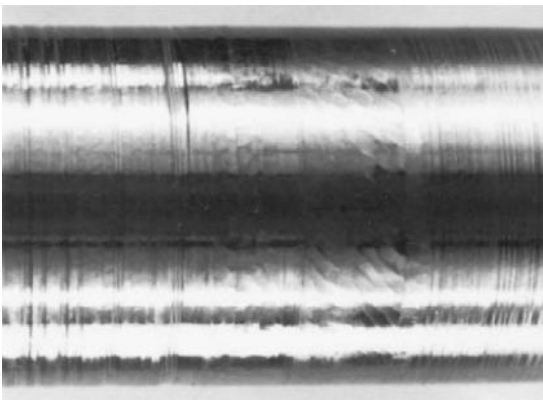


Surface defects in ultra-precision machining

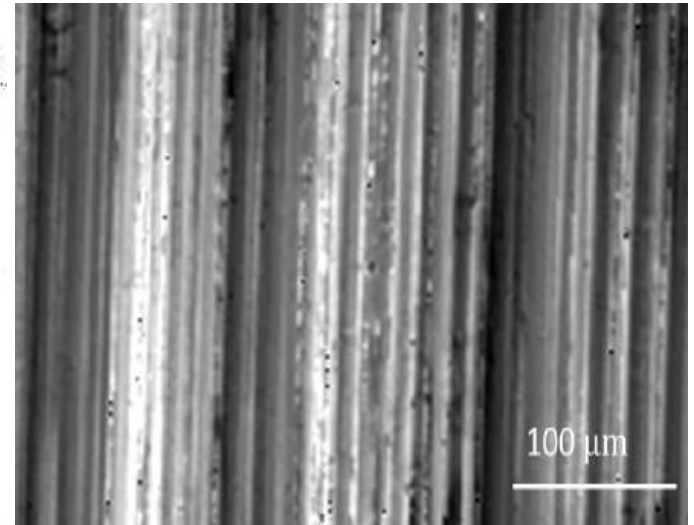
Most common surface defects (e.g. surface scratches and variations) are due to abnormal vibration (e.g. chatters) and built-up edge (BUE)

- System vibrations

- Chatter: tool, toolholder and spindle together vibrate at some natural frequency
- Scratches on the surface, ruining the geometric acquirement of product

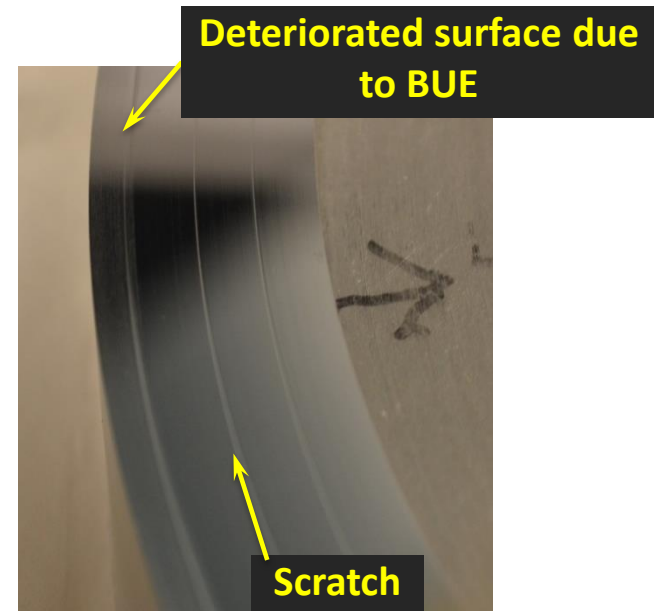
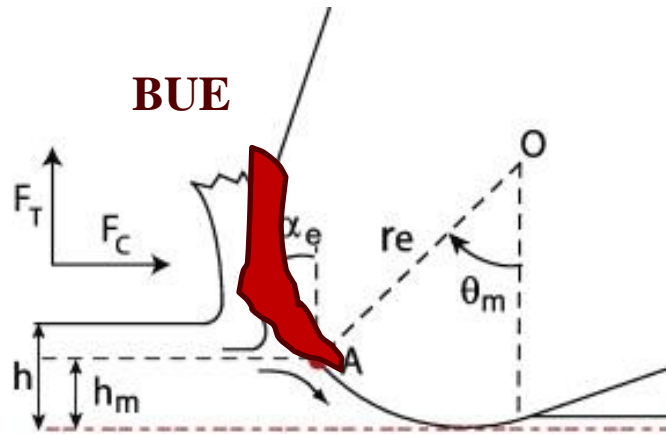


Rippled surface finish

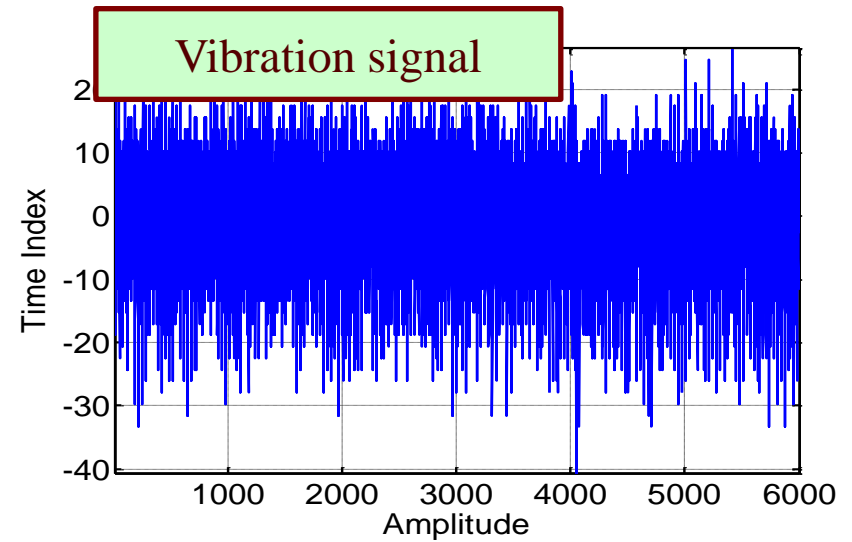
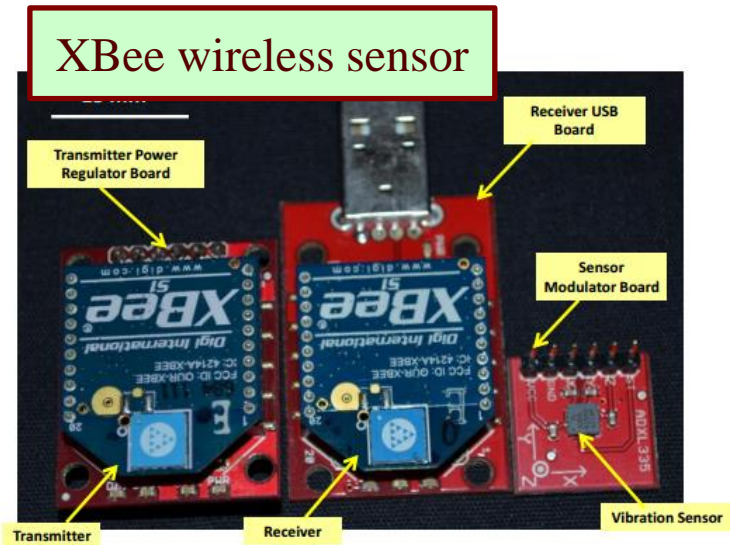
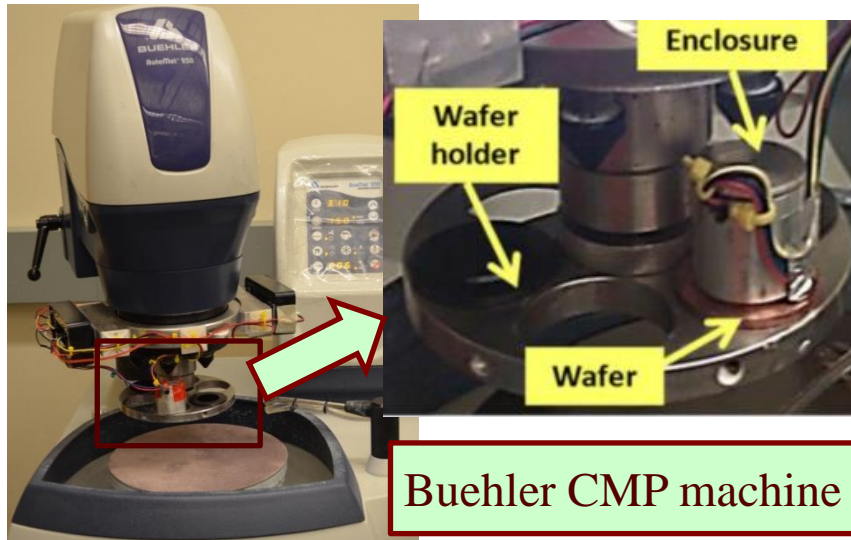


Surface defects in ultra-precision machining

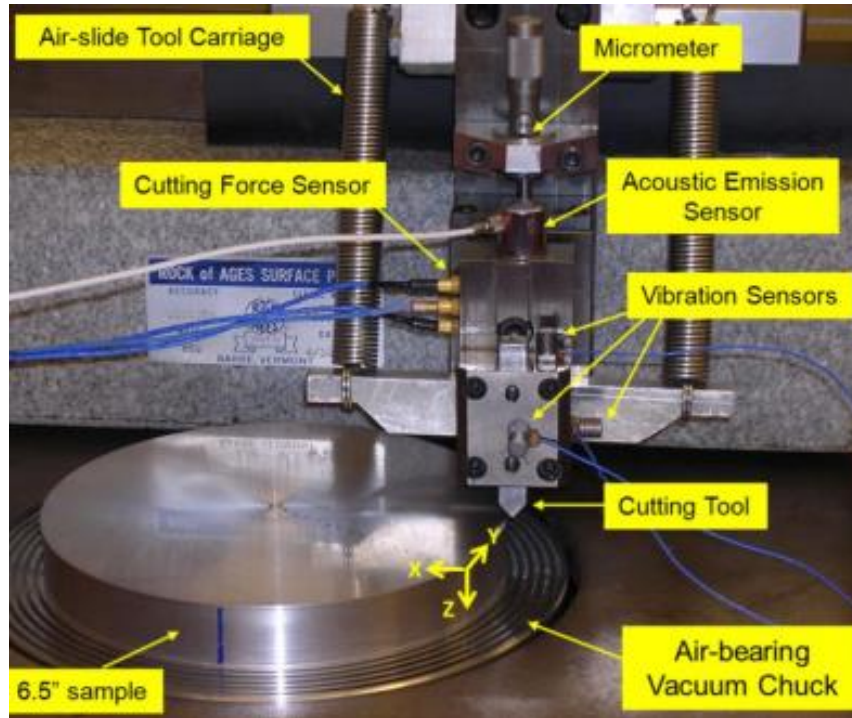
- Built-up edge (BUE)
 - Causing deeper depth of cut and degrading surface finish
 - In UPM, surface sometimes rubs against built-up edge, leading to surface quality deterioration



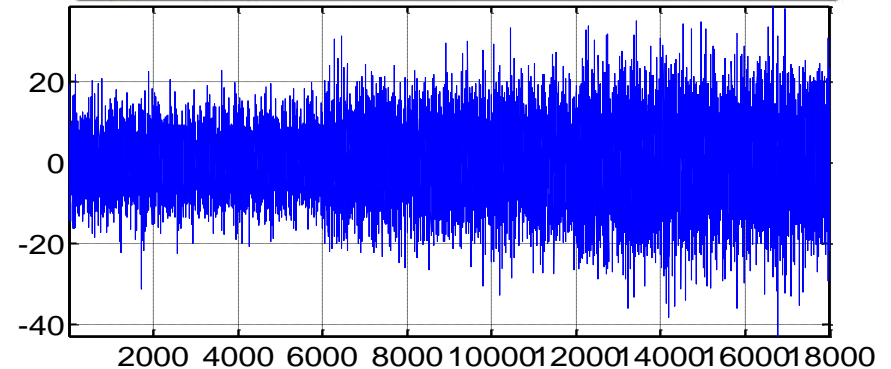
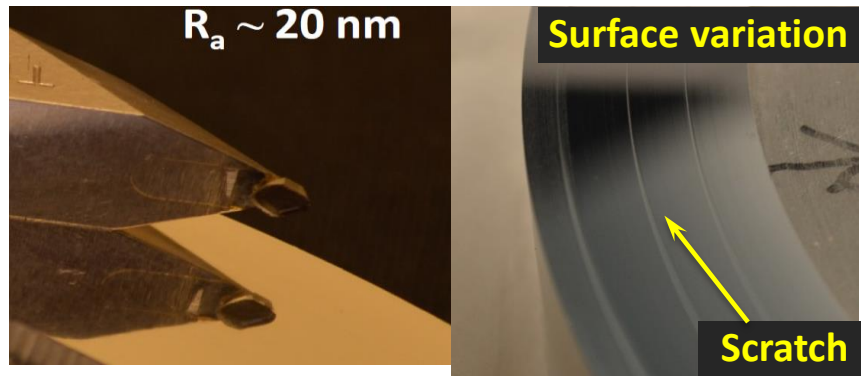
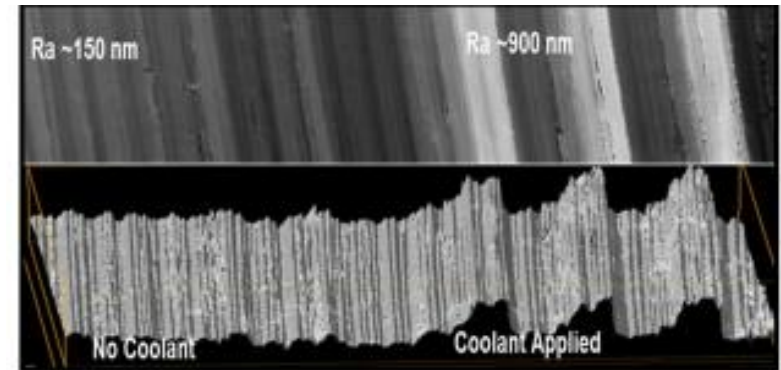
CMP experiment setup



UPM experiment setup

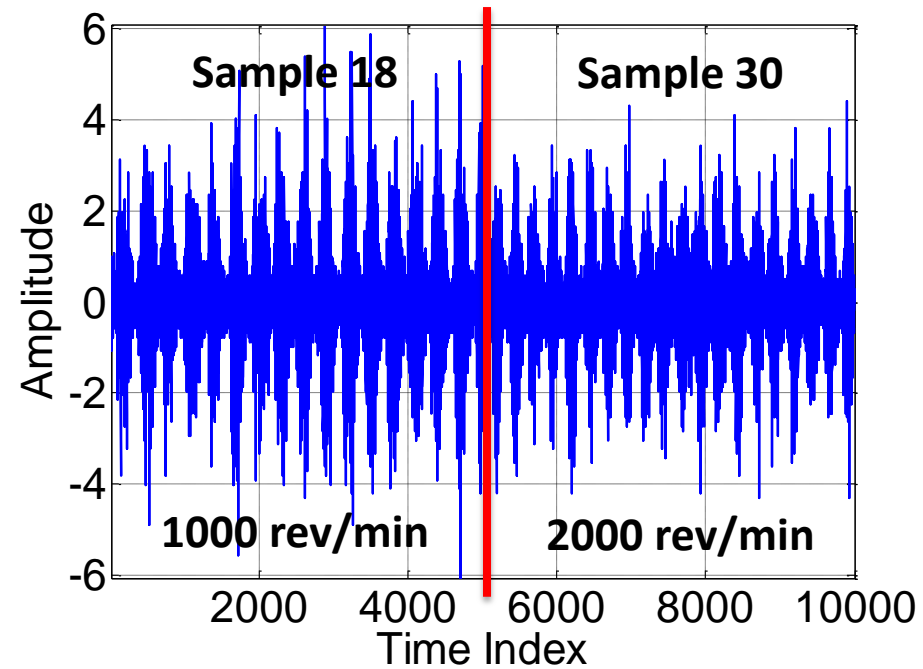
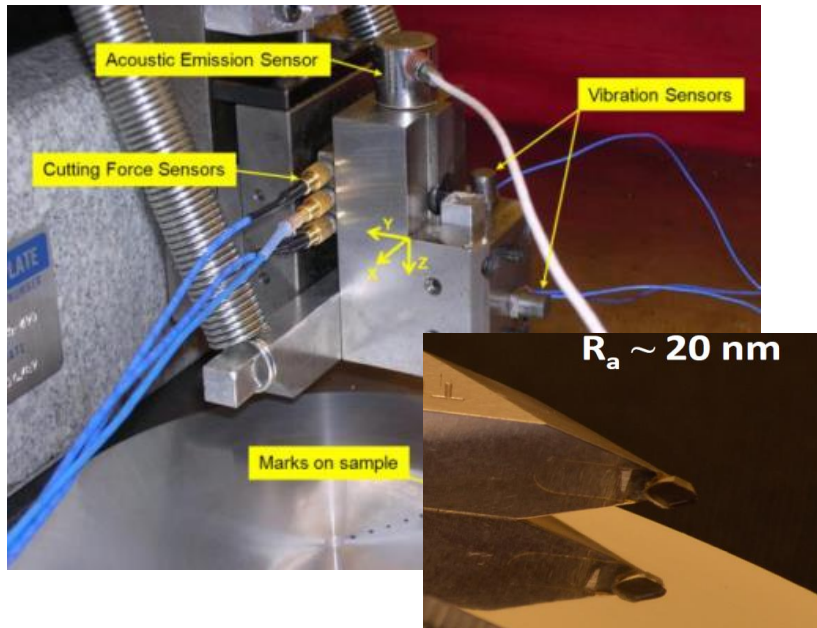


- Sensor setup
 - Vibration sensor (3-axis)
 - Force sensor (3-axis)
 - Acoustic emission (AE) sensor



Application in ultra precision machining

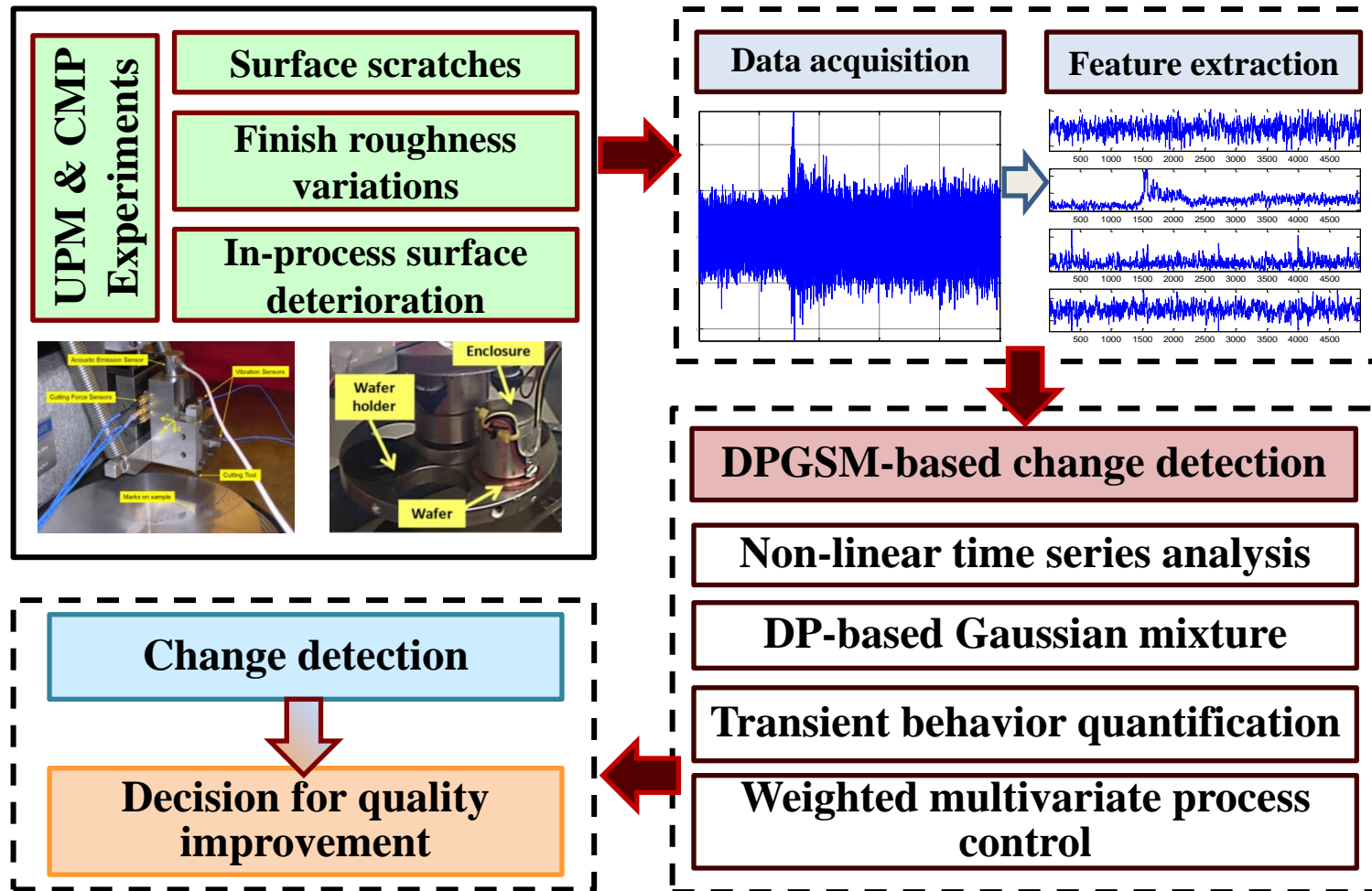
- UPM experiment
 - Depth of cut (5, 10, 20, 25 μm)
 - RPM (500, 1000, 2000 rev/min)
 - Feed rate (1.5, 3, 6 mm/min)



	1000-2000
ARL_1 of CUSUM	160
ARL_1 of EWMA	5000

SPC methods are reticent to intermittent pattern changes in UPM

DPGSM-based change detection in UPM



Limitations of traditional detection methods

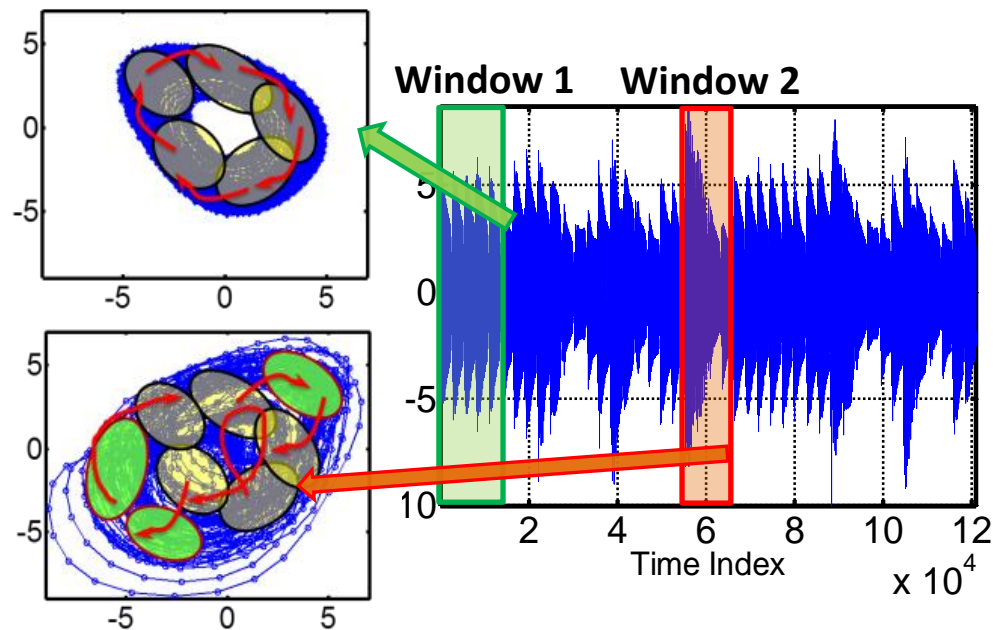
- Traditional statistical change detection involves testing a hypothesis
 - $H_0: \theta = \theta_0$ against $H_1: \theta \neq \theta_0$
 - On parameters θ of the distribution or a representation of a stochastic process, such as $x(t+1)=f(x(t), \theta)$
- For most detection methods, a stable operation implies stationarity, i.e., **θ is time-invariant**
- However, most real-world processes are highly nonstationary, i.e., **θ varies over time**

Limitations of traditional detection methods

- Autocorrelation structure change
 - Shifting trends (first order) (De Oca, 2010)
 - Volatility (second order) (Killick, 2013)
 - Eigenstructure of state space model (Basseville, 1987)
- Frequency and spectrum analysis
 - Spectral-based change detection (Choi *et al.*, 2008)
 - Wavelet based control chart (Guo, 2012)

Few methods reported for change detection in transient processes because of the difficulty to capture the complex nonstationary behaviors

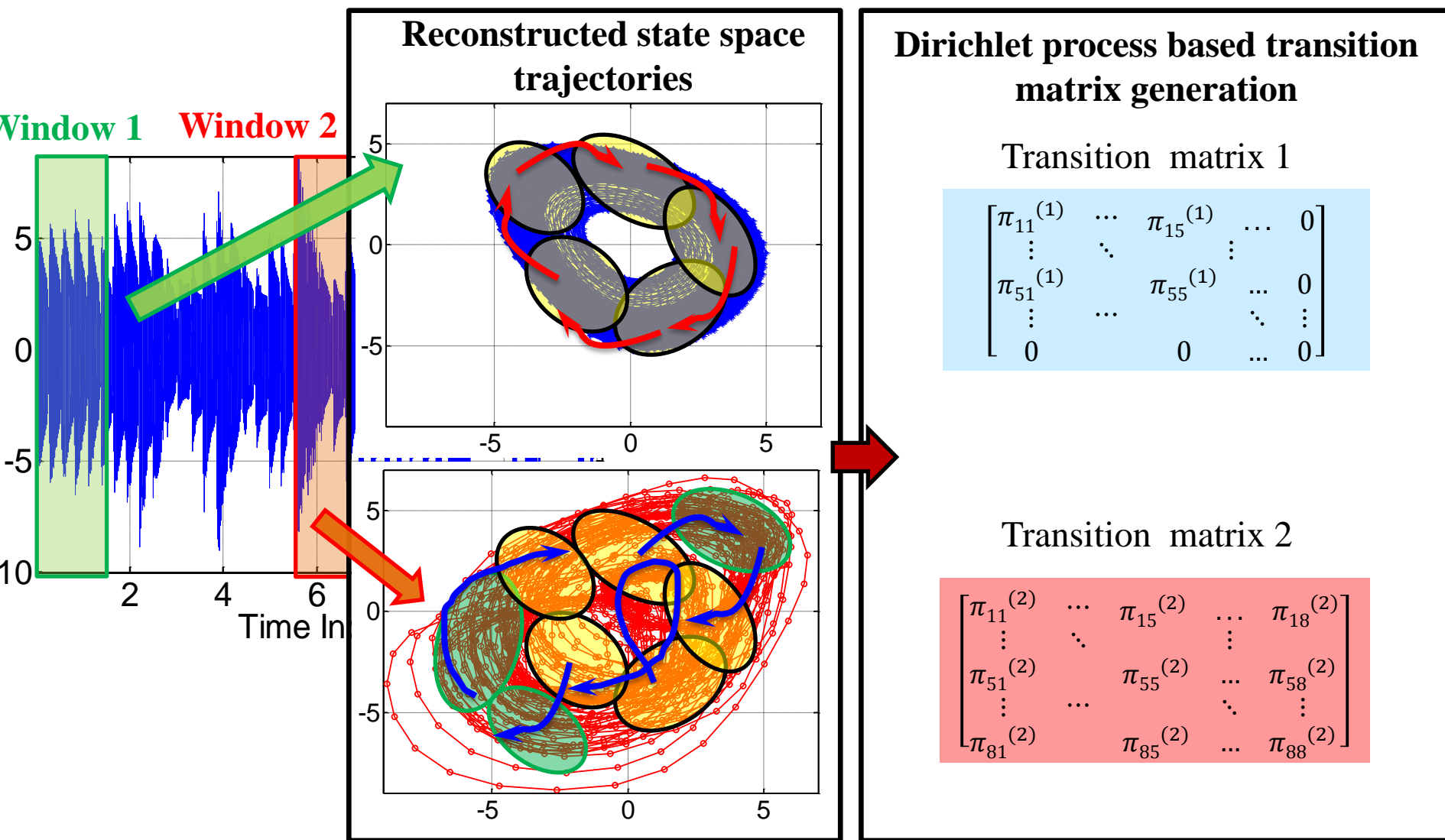
Dynamic intermittency



State space reconstructed intermittent signal

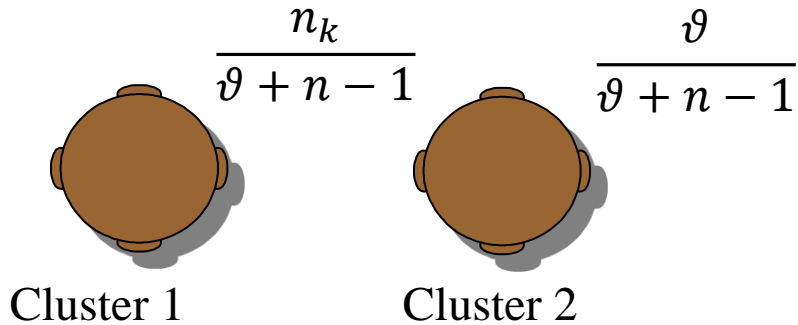
Intermittency is a common nonstationary (transient) behavior, consisting of intervals of regularity interrupted at random by bursts as the trajectory is re-injected into the chaotic part of the phase space.

Dirichlet Process-based Gaussian State Machines (DPGSM)

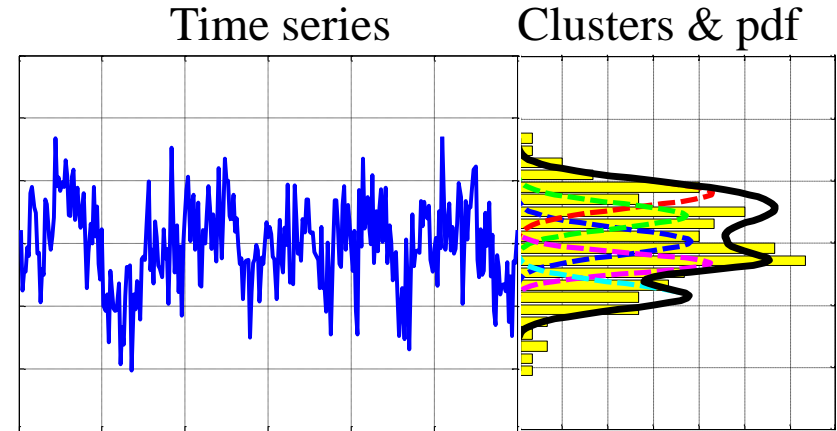


Dirichlet process-based Gaussian mixture

- Chinese restaurant process



- Tables represent infinite clusters
- Customer i represents data x_i



$$x_i \sim F(\cdot | \theta_{c_i})$$

$$\theta_{c_i} | \theta_{-c_i} \sim \frac{\sum_{\tau=1}^{i-1} \delta_{\theta_{c_i}} + \vartheta G_0}{n - 1 + \vartheta}$$

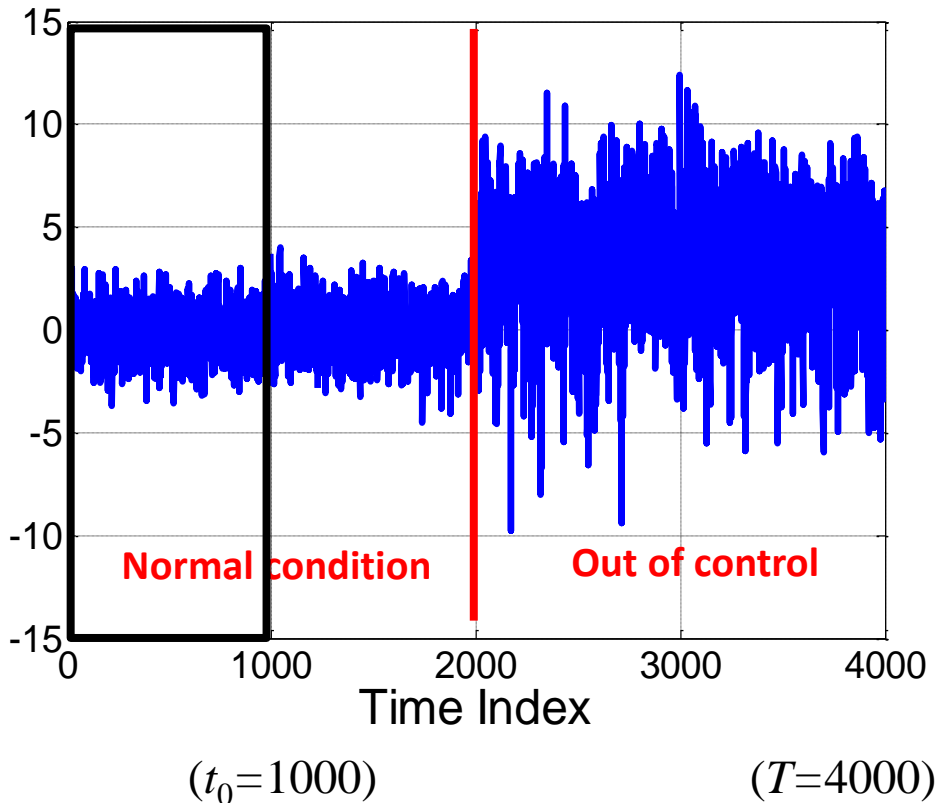


$$P(c_i = k \leq C | c_{-i}) = \frac{n_k}{n-1+\vartheta} \text{ if data belongs to existing cluster}$$

$$P(c_i = C + 1 | c_{-i}) = \frac{\vartheta}{n-1+\vartheta} \text{ if data belongs to new cluster}$$

DPGSM change detection

Simulated Data



$$\Pi^{(i)} = \{\pi_{jk}^{(i)}\} = \begin{bmatrix} \pi_{11}^{(i)} & \dots & \pi_{1K}^{(i)} \\ \vdots & \ddots & \vdots \\ \pi_{K1}^{(i)} & \dots & \pi_{KK}^{(i)} \end{bmatrix}, t_0 \leq i \leq T$$

Track the process change in terms of distribution of transition matrix

DPGSM change detection

- Distribution of transition element
 - **Proposition 1:** *The Bayesian posterior distribution of the vector $\boldsymbol{\pi}_j$, given the counts $\mathbf{Z}_j = \mathbf{z}_j^{(i)}$ (multinomial distributed), follows a Dirichlet distribution*

$$f(\boldsymbol{\pi}_j | \mathbf{z}_j^{(i)}) = \frac{1}{B(\mathbf{z}_j^{(i)})} \prod_{k=1}^K \pi_{jk}^{z_{jk}^{(i)} - 1}; \quad B(\mathbf{z}_j^{(i)}) = \frac{\prod_{k=1}^K \Gamma(z_{jk}^{(i)})}{\Gamma(\sum_{k=1}^K z_{jk}^{(i)})}$$

- Calculation of $\mathbf{z}_j^{(i)}$

$$z_{jk}^{(i)} = \sum_{t=i-L+1}^{i-1} P(c_t = j | \mathbf{x}_t, \boldsymbol{\theta}) \times P(c_{t+1} = k | \mathbf{x}_{t+1}, \boldsymbol{\theta}) + 1$$

where $P(c_t = k | \mathbf{x}_t, \boldsymbol{\theta}) = b f(\mathbf{x}_t | \theta_k)$, b is an appropriate normalized constant

which makes
$$\sum_{k=1}^K b f(\mathbf{x}_t | \theta_k) = 1$$

Multivariate control chart

- Confidential level
 - In DPGSM change detection, we have K control charts (K as cluster number)
 - $\alpha_j = 1 - (1 - \alpha)^{\frac{w_j}{K}}$ is the significance level of row j , set by the family-wise error rate ($FWER$), i.e. $FWER = Pr(\text{rejecting at least one } H_j | H_j \in H_0) = \alpha$, where $H_0 = \{H_1, H_2, \dots, H_K\}$
- Measurement in multivariate control chart
 - $\bar{\pi}_{jk} = \pi_{jk} | \mathbf{z}_j^{(i)} = \frac{z_{jk}^{(i)}}{\sum_{k=1}^K z_{jk}^{(i)}}$
 - $d_j^2 = (\bar{\boldsymbol{\pi}}_j - \boldsymbol{\pi}_{j0}) \mathbf{S}_j^{-1} (\bar{\boldsymbol{\pi}}_j - \boldsymbol{\pi}_{j0})^T \sim \chi^2_K$ distribution

Multivariate control chart

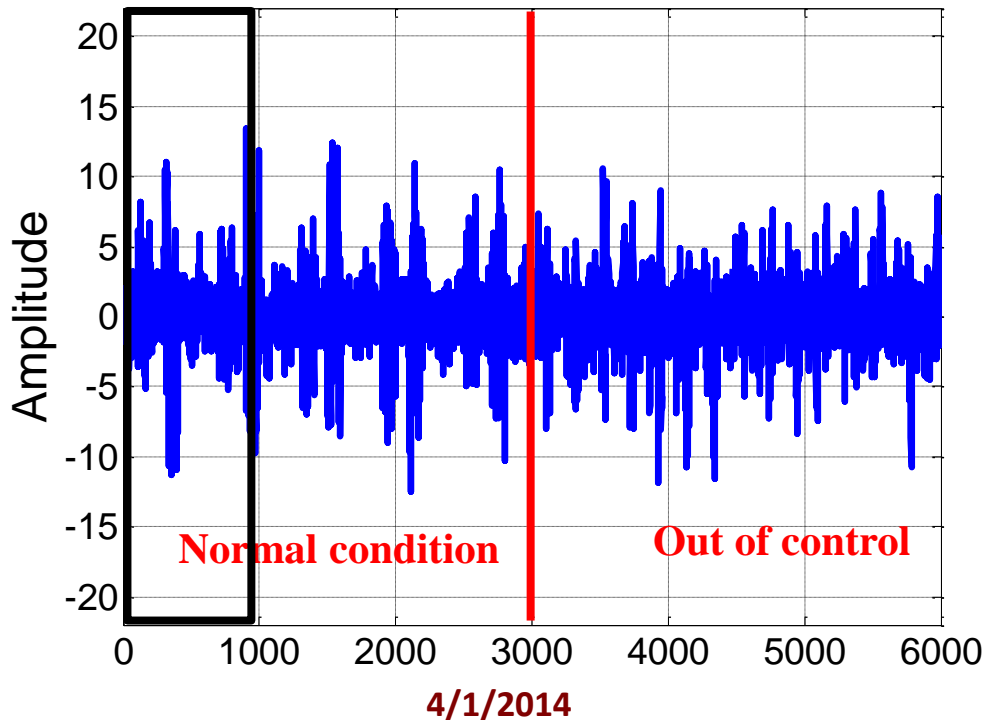
The overall on-line change detection, after consistent estimation of Θ , $\{UCL_j\}$ and α based on a training set, may be summarized as follows:

Step 1: Estimate transition matrix: $\bar{\pi}_{jk} | z_j^{(i)} = \frac{z_{jk}^{(i)}}{\sum_{k=1}^K z_{jk}^{(i)}}$

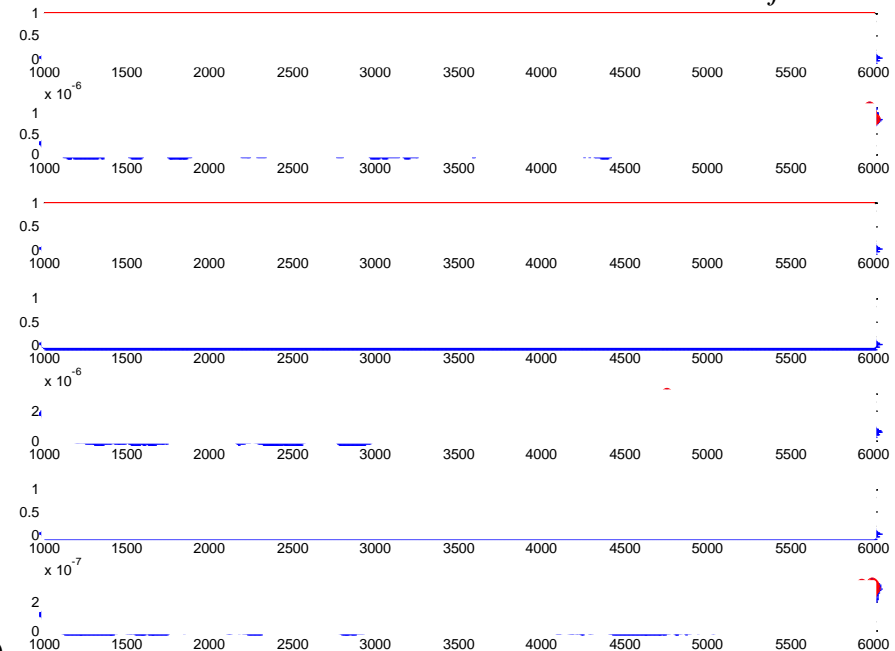
Step 2: Calculate Hotelling statistics d_j^2 for each row j

Step 3: Monitor the process and estimate ARL_1 based on out-of-control points

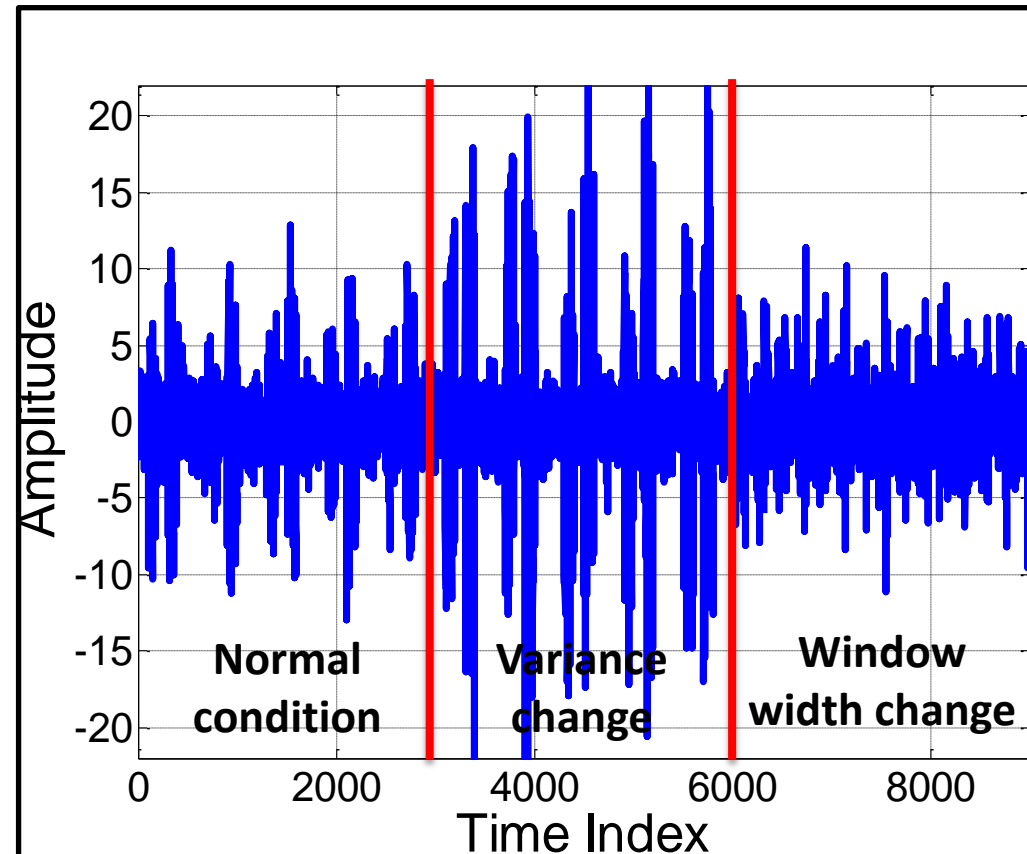
Simulated Data



Control Chart for transition row π_j



Benchmark case



ARMA(2,1) model $a_t \sim (N(0, \delta\sigma_a^2))$

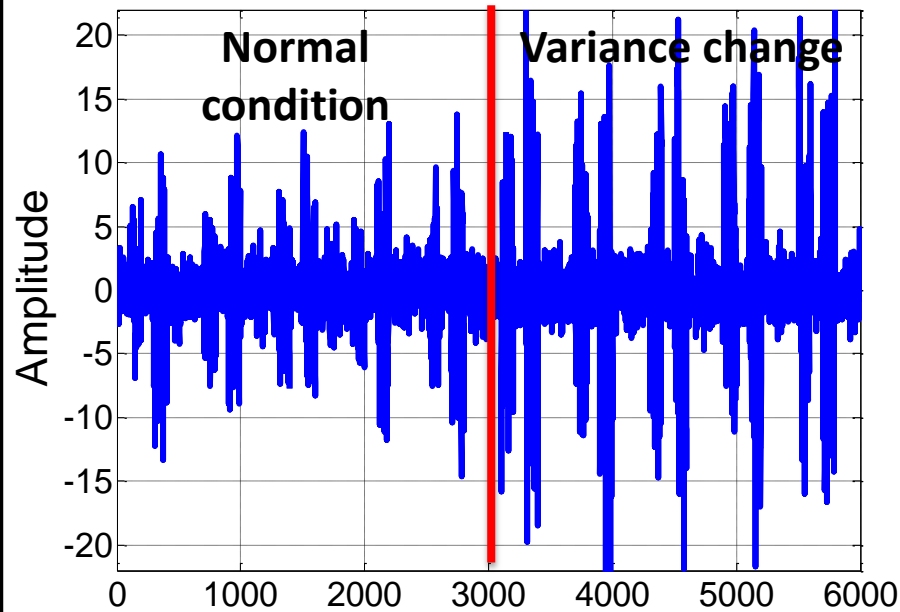
Model:

$$x_i = \begin{cases} f(x_{-i}; \boldsymbol{\varphi}^{(1)}, \boldsymbol{\psi}^{(1)}) & i_0 < i < i_1 \\ \dots & \dots \\ f(x_{-i}; \boldsymbol{\varphi}^{(m)}, \boldsymbol{\psi}^{(m)}) & i_{m-1} < i < i_m \\ \dots & \dots \\ f(x_{-i}; \boldsymbol{\varphi}^{(M)}, \boldsymbol{\psi}^{(M)}) & i_{M-1} < i < i_M \end{cases}$$

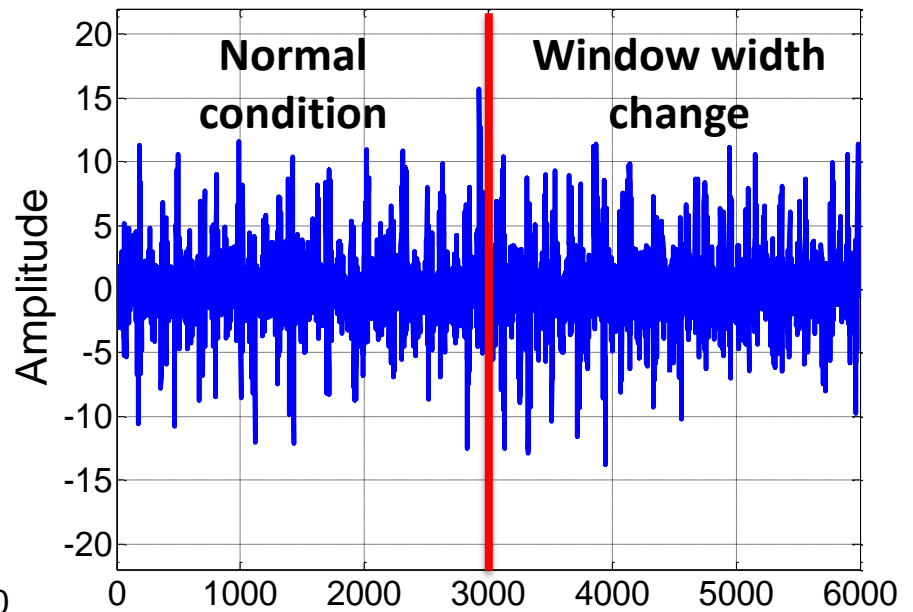
where i_m is the time index of each breakpoint, $m=1, 2, \dots, M$, $i_0 = 1$, $i_M = N$ (N is the length of the time series).

$\{i_0, i_1, \dots, i_m, \dots, i_M\}$ as a sequence of order statistics such that each i_m follows a uniform distribution $UNIF(0, N)$.

Benchmark case



Fault A: variance change



Fault B: sojourn time change

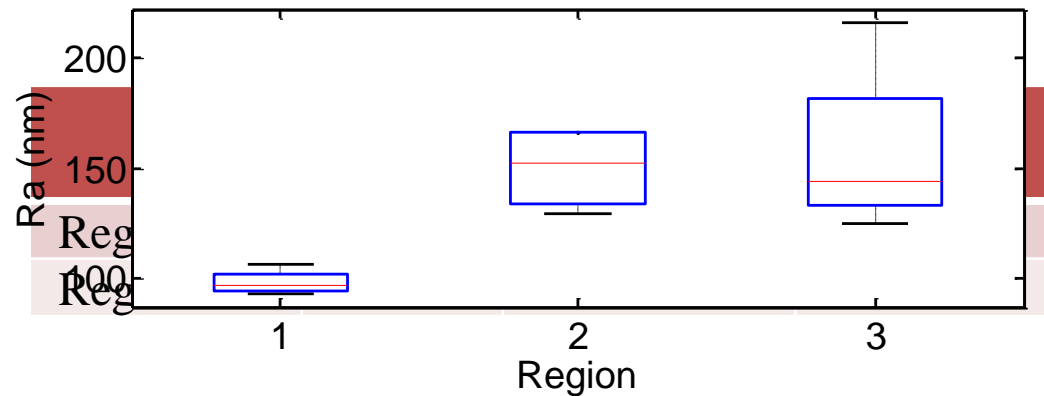
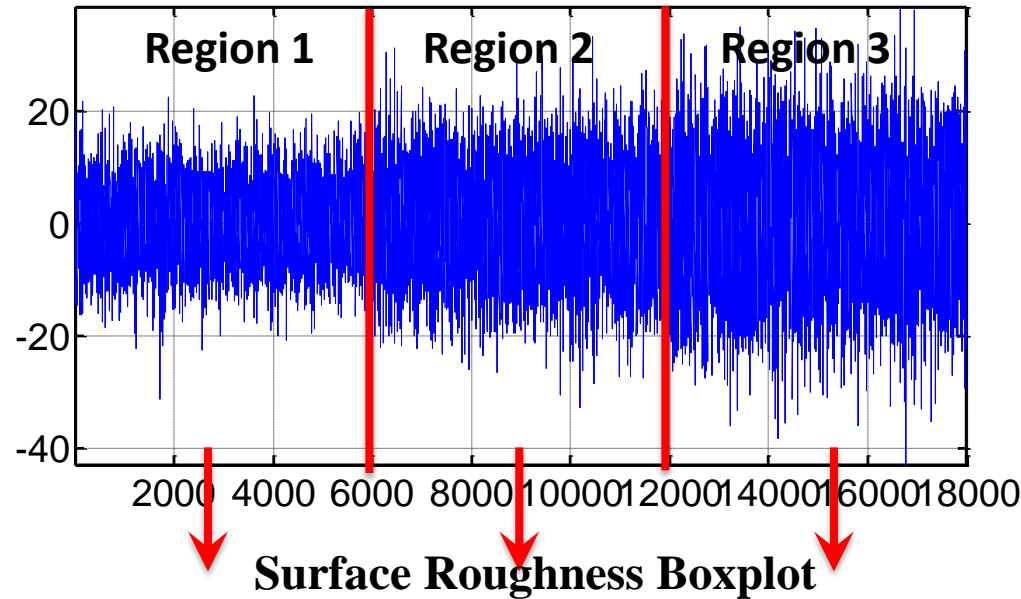
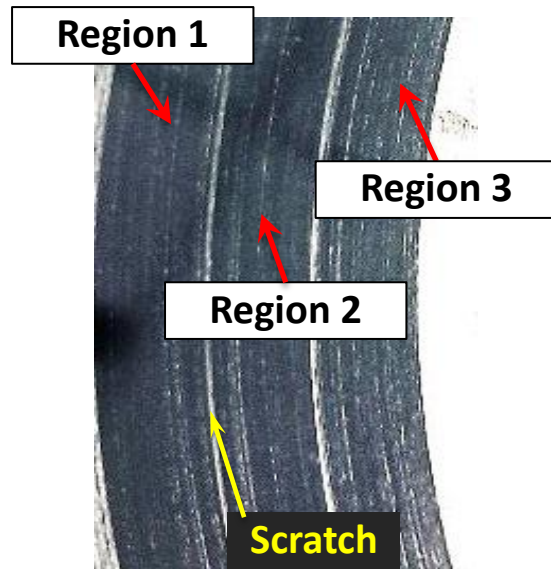
ARL_1 comparisons (expected steps to reveal a change)

	EWMA	SD-WCUSUM	RNDP	DPGSM
Fault A	25.6	2.2	6.1	3.5
Fault B	Inf	Inf	Inf	3.8

Detection for surface roughness variation

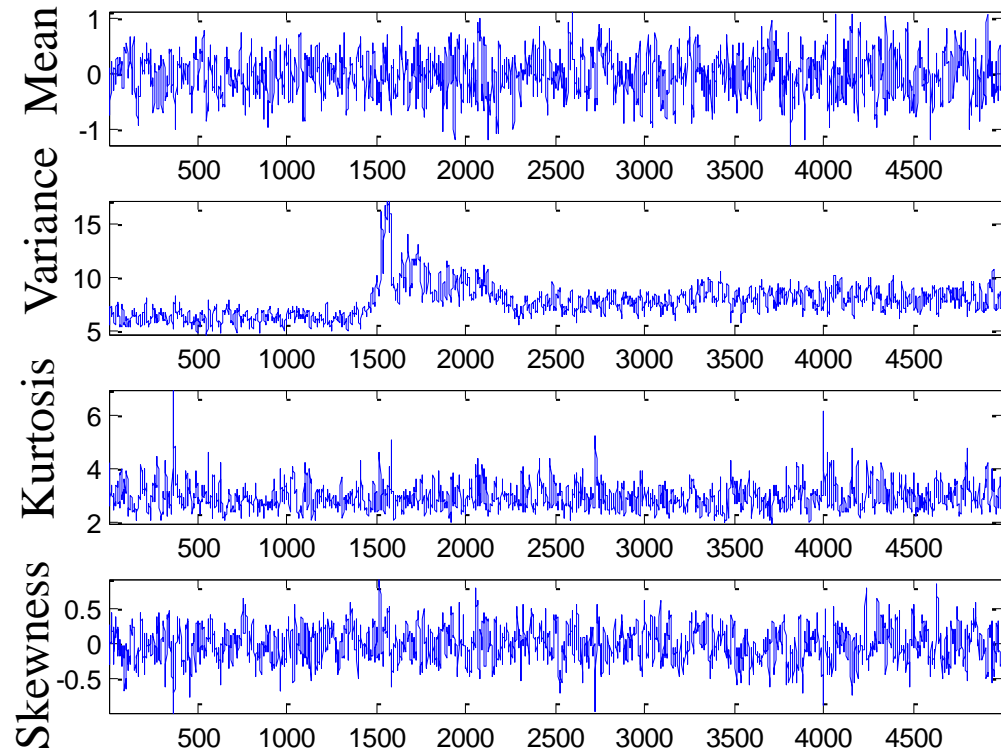
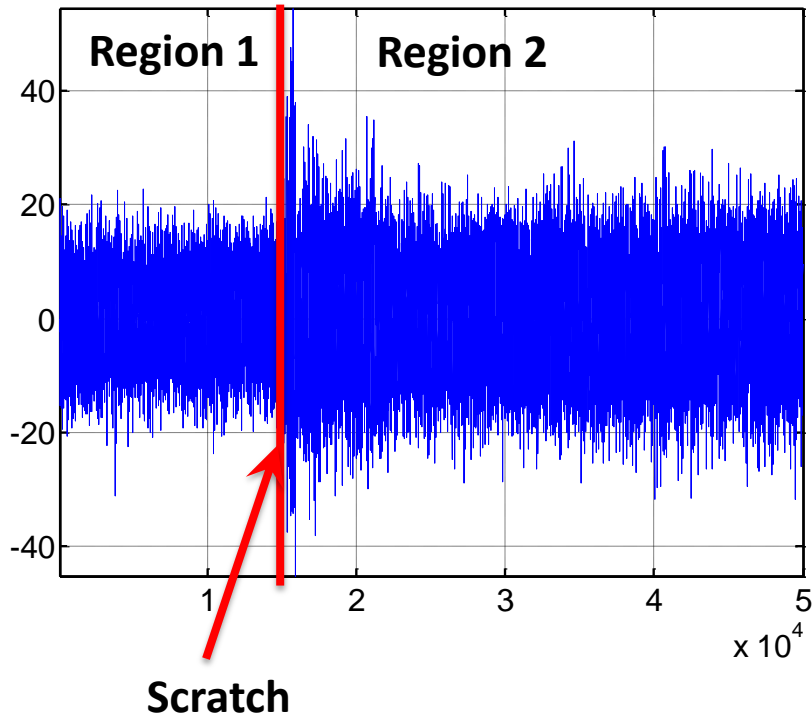
- Surface variation in three regions

- Small Ra ($\sim 100\text{nm}$)
- High Ra ($\sim 150\text{nm}$)
- High Ra ($\sim 150\text{nm}$) with larger variance

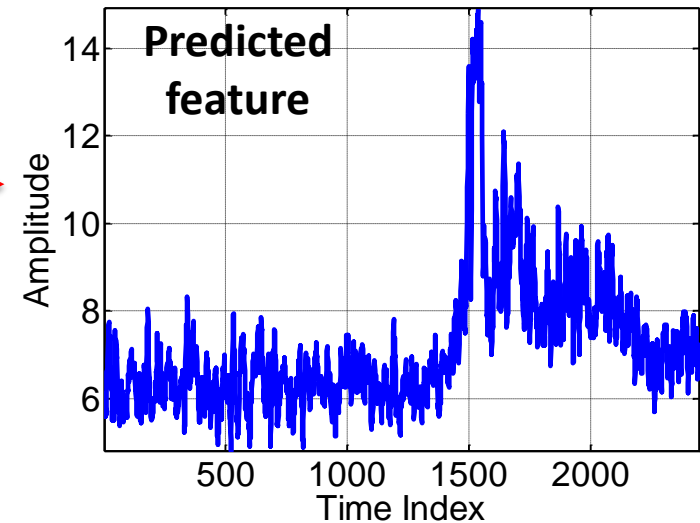
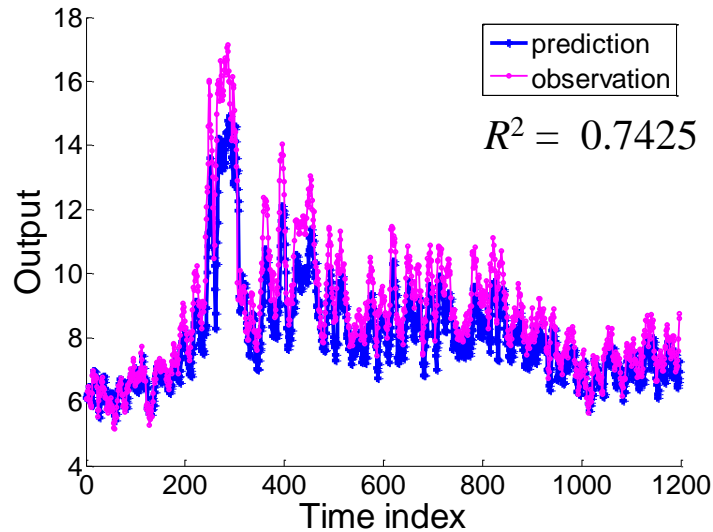


Detection for surface scratch

- Surface scratch and vibration signal



Detection for surface scratch



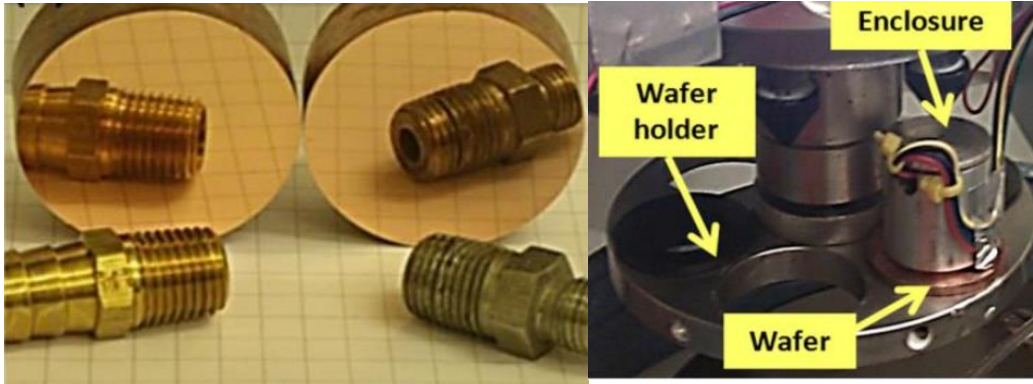
Expected delay of detection(ms) comparisons

EWMA	SD-WCUSUM	DPGSM
164	72	24

GP-DPGSM method discovers scratch appearance in 48 *ms* ahead of EWMA and 140 *ms* earlier than SD-WCUSUM.

Change detection of surface deterioration

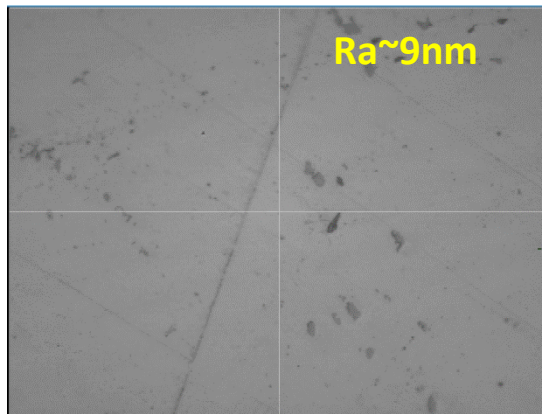
- Chemical Mechanical Planarization (CMP) process experiment
 - Lapped coppers (Ra 10nm~15nm) were polished on Buehler in 3 minutes of each interval
 - Platen speed 250 RPM, head speed 60 RPM and download force 4 lbs



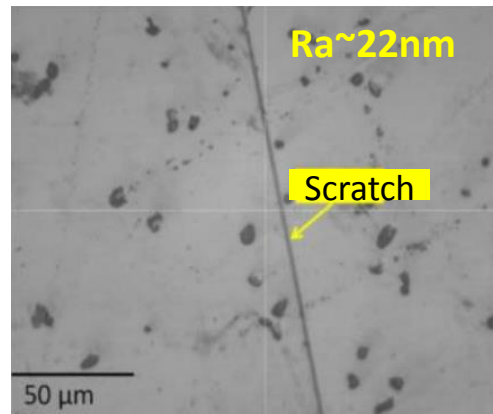
Buehler (model Automet[®] 250) with 3-axis accelerometer

Change detection of surface deterioration

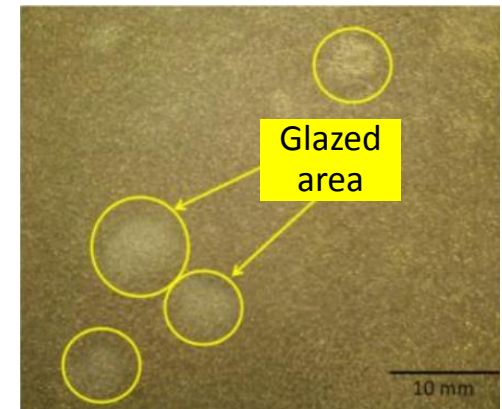
- Pad wear and surface deterioration
 - After 3 minutes, the average Ra improved to around 15 nm
 - Pad wear was then accelerated worn by soaking the pad in slurry, followed by air drying
 - After 12 minutes polishing, it was noticed that significant glazing of polishing pad observed (Fig. 2) as well as the scratch on wafer were observed and finish degrades to $Ra \sim 22\text{nm}$



After 3 min

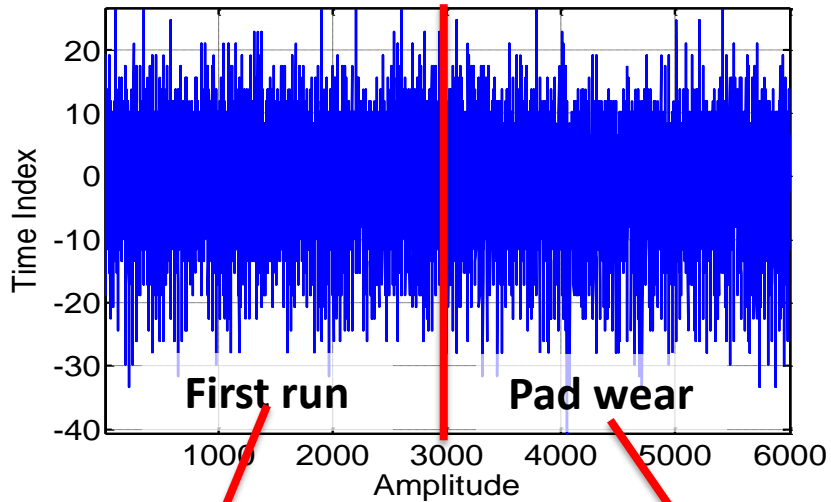


After 12 min



Glazed areas on pad

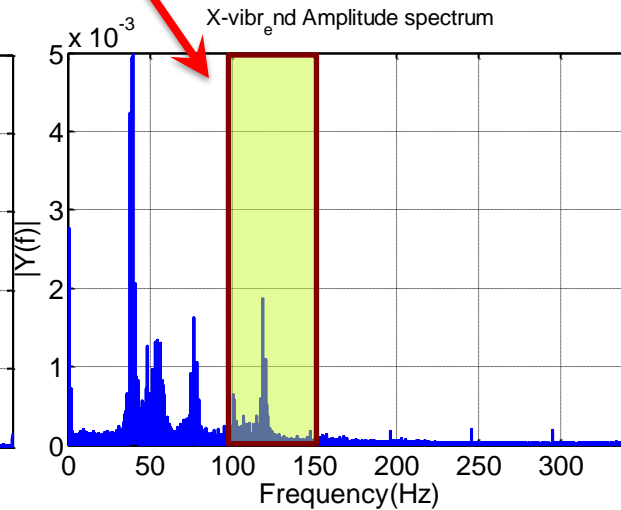
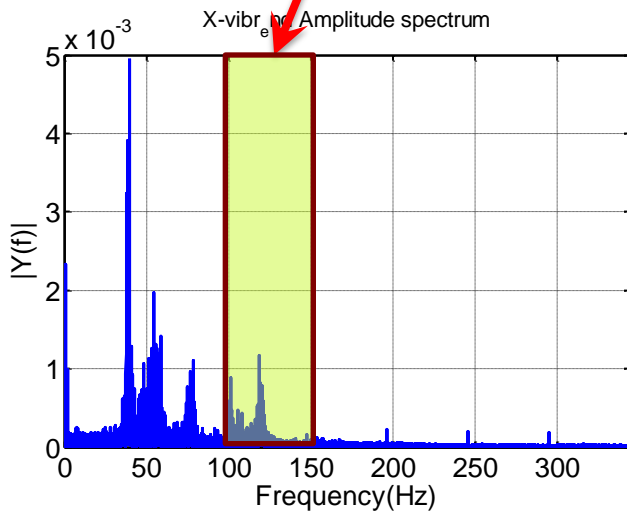
Change detection of surface deterioration



Delay for detection (ms)

EWMA	SD-WCUSUM	DPGSM
2941	2262	34

DPGSM discovers surface deterioration with an order of magnitude (more than 2 sec) earlier than SPC methods tested



Change detection for music pattern changes

- Case 1



Normal condition E5 to D5 Key signature change

- Case 2



Normal condition: 1 1 1 2 2 2

Anomaly condition: 1 1 2 2 1 2

Comparison of delays for change detection (ms)

	EWMA	SD-WCUSUM	DPGSM
Key signature change	90	5	2
Chord progression change in long period articulation	83	175	15

Change detection in Ragas

Change detection 1: Sequence change with ascending and descending scales

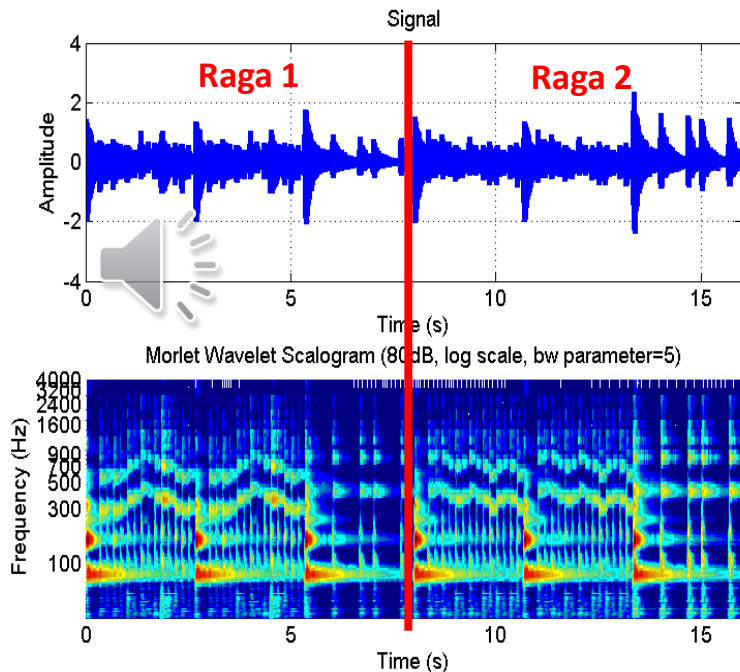
Change detection 2: Scale change with missing notes

	C	D \flat	D	E \flat	E	F	F \sharp	G	A \flat	A	B \flat	B
YamanK.	•		•		•	•	•	•		•		•
Yaman	•		•		•		•	•		•		•
MaruBihag	•		•		•	•		•		•		•
GaudSarang	•		•		•	•		•		•		•
Hameer	•		•		•	•		•		•		•
Desh	•		•		•	•		•		•		•
TilakKamod	•		•		•	•		•		•		•
GaudMalhar	•		•		•	•		•		•	•	•
Jaijaiwante	•		•		•	•		•		•	•	•
Khamaj	•		•		•	•		•		•	•	•
Bihag	•		•		•	•	•	•		•		•
Kedar	•		•		•	•	•	•		•	•	•
Rageshri	•		•		•	•				•	•	
Bageshri	•		•	•		•		•		•	•	
Bhimpalasi	•		•	•		•		•		•	•	

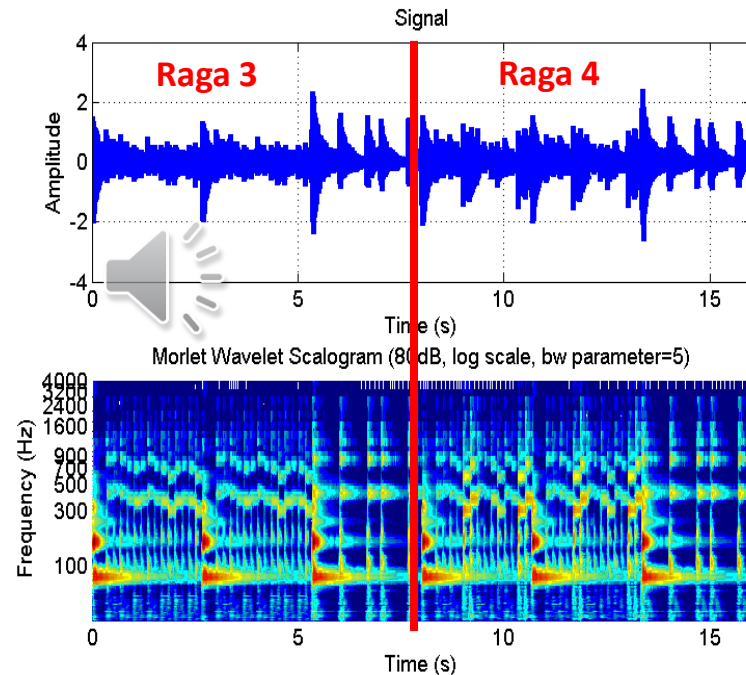
General types of Raga music

Subtle changes in intermittent music signals, namely **scores sequence change** and **music scale change**, are considered.

Change detection in Ragas



Ascending and descending scales



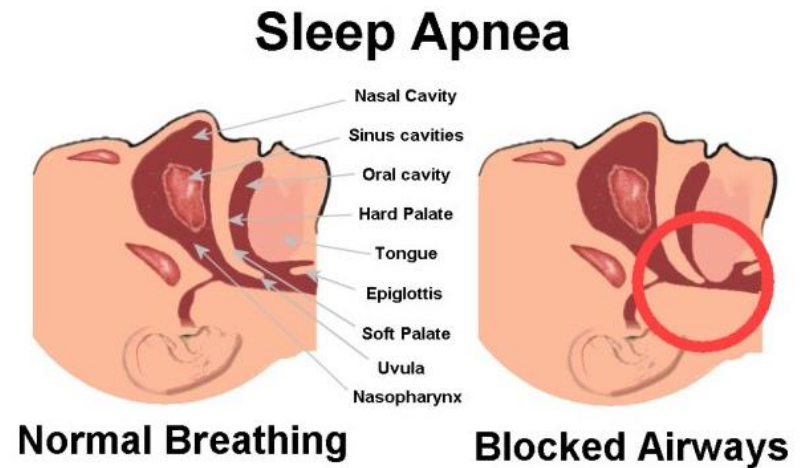
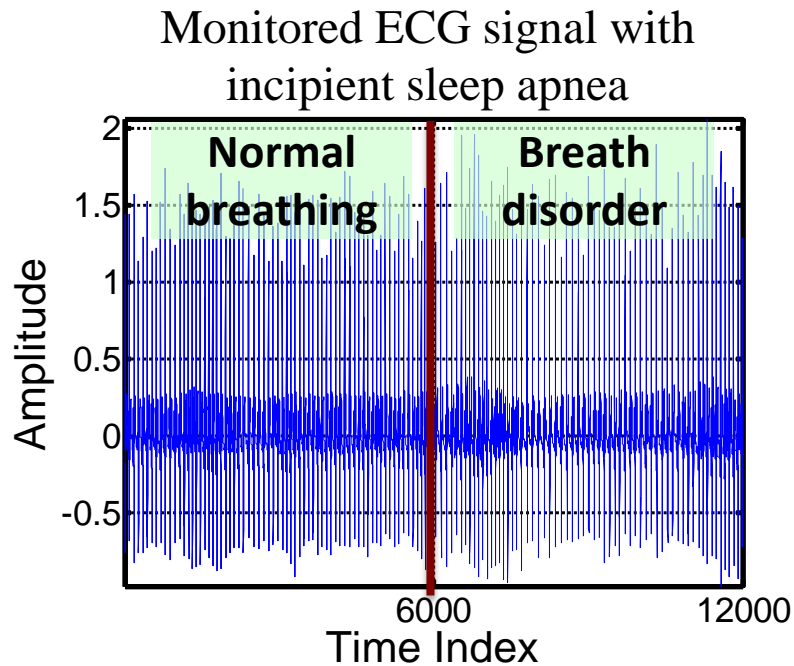
Scale change with missing notes

Comparison of delays for change detection (ms)

	EWMA	SD-WCUSUM	DPGSM
Ascending and descending scale	24(False alarm)	Inf	17
Descending scale with missing note	1682	191	151

Detection of incipient sleep apnea

- Sleep apnea detection using ECG signal



Delay for detection (ms) of sleep apnea

EWMA	SD-WCUSUM	DPGSM
1765	12	11

Conclusions

- We represent nonlinear nonstationary (intermittency) signal within precision machining processes as **a stochastic mixture of Gaussian clusters with Markov transition matrix**
- Intermittent changes in surface uniformity are efficiently identified by DPGSM, and it could detect surface damage (scratch) almost an order of magnitude earlier compared to existing change detection methods (EWMA and SD-WCUSUM)

Further studies

- **Parameters selection**
 - Selection of **window length L** is crucial to derive consistent estimates of the transition matrix elements
 - Selection of the **concentration parameter ϑ** of Dirichlet process to ensure generation of proper Gaussian mixtures
- The transition process may be more closely approximated using a **semi-Markov formulation** and the representation needs to be modified to better capture the underlying dynamics

Q & A

Contact me:

Zimo Wang

Ph.D. candidate

Industrial Engineering

zimo.wang.1987@gmail.com